Generation of Intense High-Order Vortex Harmonics

Xiaomei Zhang,[1] Baifei Shen,[1,2,*] Yin Shi,[1] Xiaofeng Wang,[1] Lingang Zhang,[1] Wenpeng Wang,[1] Jiancai Xu,[1] Longqiong Yi,[1] and Zhizhan Xu[1]

[1]*State Key Laboratory of High Field Laser Physics, Shanghai Institute of Optics and Fine Mechanics, Chinese Academy of Sciences, Shanghai 201800, China*

[2]*IFSA Collaborative Innovation Center, Shanghai Jiao Tong University, Shanghai 200240, China*

(Received 9 October 2014; published 28 April 2015)

This Letter presents for the first time a scheme to generate *intense* high-order optical vortices that carry orbital angular momentum in the extreme ultraviolet region based on relativistic harmonics from the surface of a solid target. In the three-dimensional particle-in-cell simulation, the high-order harmonics of the high-order vortex mode is generated in both reflected and transmitted light beams when a linearly polarized Laguerre-Gaussian laser pulse impinges on a solid foil. The azimuthal mode of the harmonics scales with its order. The intensity of the high-order vortex harmonics is close to the relativistic region, with the pulse duration down to attosecond scale. The obtained intense vortex beam possesses the combined properties of fine transversal structure due to the high-order mode and the fine longitudinal structure due to the short wavelength of the high-order harmonics. In addition to the application in high-resolution detection in both spatial and temporal scales, it also presents new opportunities in the intense vortex required fields, such as the inner shell ionization process and high energy twisted photons generation by Thomson scattering of such an intense vortex beam off relativistic electrons.

DOI: 10.1103/PhysRevLett.114.173901 PACS numbers: 42.65.Ky, 42.50.Tx, 52.38.-r

Light beams can exhibit helical wave fronts: the light phase "winds up" around the spatial beam center and forms an optical vortex. The phase wind imprints an orbital angular momentum (OAM) to the beam [1,2]. The characteristic helical phase profiles of optical vortices are described by $\exp(il\phi)$ multipliers, where ϕ is the azimuthal coordinate and the integer number l is their topological charge, corresponding to the order of the mode. The total phase accumulated in one full annular loop is $2\pi l$, and an OAM of $l\hbar$ is carried by per photon for an l-order linearly polarized optical vortex beam. Based on this, the high-order optical vortex beam provides a powerful tool in optical information to investigate the entanglement state [3] and for studies of cold atoms and enhancing atomic transition [4–7].

In order to provide more quantum information and for other potential applications, high-order vortex beams are required. However, limited by the etching resolution, the common method using forked diffraction grating [8] or the spiral phase plates [1] to generate the optical vortex beams is difficult to be used to obtain them. Many studies have attempted to generate light beams with OAM. For example, a relativistic electron beam can act as a mode converter that interacts with a laser in a helical undulator [9–11] and high-energy photons in MeV-GeV with OAM can be obtained by Compton backscattering of twisted laser photons off relativistic electrons [12], where the mode of the Laguerre-Gaussian (LG) pulse remains unchanged. In addition, in view of the gas high-order harmonics generation (HHG) scheme [13–15], because of the confluence of OAM and HHG, this scheme has an extraordinarily promising perspective. The observed harmonics possess a helical wave front in both experimental [16,17] and theoretical studies [18,19] when a $\sim 10^{15}$ W/cm^2 helical beam is focused into a gas jet. Although some debate exists on how OAM is transferred to high-order harmonics between the first experimental [16] and theoretical [18] studies (the bifurcation is that the topological charge of high-order harmonics would be equal to that of the fundamental or not), the recent inspiring report [17] confirms the accordance of the model and experimental results.

While those interesting findings are expected to be studied more in the future, in this Letter, we present the first way to generate intense high-order helical beams in the extreme ultraviolet (XUV) region using plasma as the mode converter. When an intense linearly polarized driving vortex beam with low-order mode impinges on a solid target, both the reflected and transmitted light include high-order harmonics, the phase of which scales with the harmonic order. In this nonlinear process, OAM carried by the driving helical light is readily transferred to the harmonics. The azimuthal mode of the generated optical vertex beam can easily reach over ten or even a few tens. Moreover, plasma as the nonlinear medium shows superiority in the damage threshold compared with the optical component. With the present scheme, the intensity of the generated high-order vortices is close to the relativistic region. In addition, such a generated beam is ultrashort (attosecond) in time scale, making it an ideal tool for probing electronic dynamics on the atomic or molecular scale. Our scheme may for the first time produce a vortex

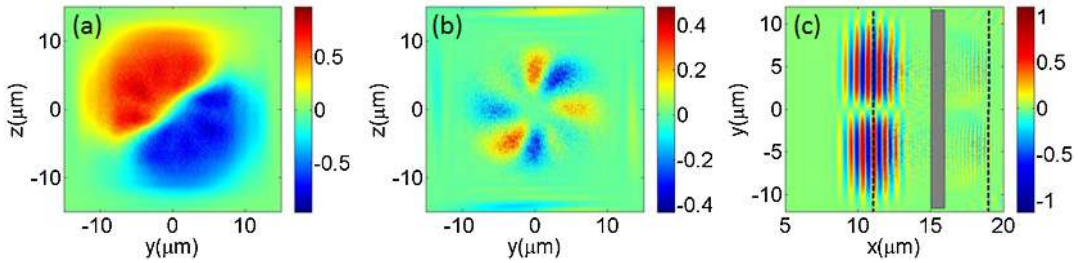

FIG. 1 (color online). (a) Electric field E_y of the reflected pulse in the $z-y$ plane at $x = 11$ μm, (b) electric field E_y of the transmitted pulse in the $z-y$ plane at $x = 19$ μm, and (c) total electric field E_y in the $x-y$ plane at $z = 0$ μm at $t = 74.7$ fs when the incident LG_{10} beam is completely reflected from the solid target. The black dotted lines in (c) show the x positions of planes in (a) and (b), and the gray box shows the foil position. The field is normalized to $m_e\omega_0 c/e(4\times10^{12}$ V/m).

pulse simultaneously of the high intensity, short wavelength, and high-order modes. Such an intense vortex beam will present new opportunities for applications in intense vortex required fields such as the inner shell ionization process and high energy twisted photons generation by Thomson scattering of such intense vortex beams off relativistic electrons, and for high-resolution detection in both spatial and temporal scales.

The proposed scheme is confirmed with three-dimensional (3D) particle-in-cell (PIC) simulations based on the VORPAL code. The driving LG beam is p polarized, described as

$$a(\mathrm{LG}_{lp}) = a_0\left(\frac{\sqrt{2}r}{r_0}\right)^l \exp\left(-\frac{r^2}{r_0^2}\right)\exp(il\phi)(-1)^p \times L_p^l\left(\frac{2r^2}{r_0^2}\right)\sin^2\left(\frac{\pi t}{2t_0}\right). \quad (1)$$

In this simulation, $l = 1$, $p = 0$ meaning the LG_{10} beam (low-order optical vortex mode) is used, $r_0 = 6$ μm and $t_0 = 3T$, where T is the driving laser period and ϕ is the azimuthal coordinate (relating to the positon of y, z) within the range of $[0\,2\pi]$. For the laser wavelength $\lambda_0 = 0.8$ μm, $a_0 = eA/m_e c^2 = 2$, corresponds to a peak electric field intensity 4×10^{12} V/cm, where A is the vector potential, c is the light speed in vacuum, m_e is the electron mass, and e is the electron charge. The thin foil as the nonlinear converter occupies the region 15 μm $< x <$ 16 μm in the propagation direction of the driving beam and -12 μm $< y(z) <$ 12 μm in the transverse direction with a density of $n_0 = 1\times10^{22}/\mathrm{cm}^3$. The simulation box is 20 μm$(x)\times$ 24 μm$(y)\times$ 24 μm(z), which corresponds to a window with $1000\times400\times400$ cells and two particles per cell. At $t = 0$, the laser pulse enters the simulation box from the left boundary.

Figure 1 shows the electric field distributions of the reflected and transmitted pulses in the $z-y$ plane when the driving beam is completely reflected from the solid foil [see Fig. 1(c)]. A comparison of Figs. 1(a) and 1(b) shows that the mode of the transmitted field has a complicated structure that may contain high-order LG-like modes, whereas the transverse plane of the reflected field still shows the LG_{10} mode like the driving field. To see the information of harmonics modes more clearly, we plot the transverse electric field distributions of the third, fifth, seventh, and ninth harmonics of the reflected field in Fig. 2, and the harmonic mode can then be seen clearly. According to the number of intertwined helices, the corresponding azimuthal modes of these harmonics are $l = 3$, 5, 7, 9, respectively. The Supplemental Material (reflected electric field distribution of the third harmonic in the $z-y$ plane by changing the x position from $x = 10.8$ to $x = 11.54$ μm with $\Delta x = 0.02$ μm) clearly and intuitively shows the helical feature [20]. The distance of rotating one loop of E_y is approximately $\lambda_3 = 0.2667$ μm, which is just equal to the wavelength of the third harmonics $\lambda_0/3$. Seeing from the frequency spectrum, we know that the expected harmonics information in Fig. 1(a) is covered because of the much higher intensity of the fundamental field, that is,

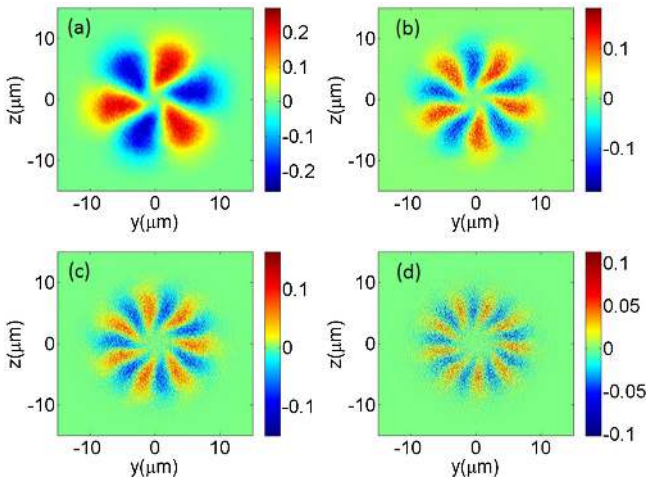

FIG. 2 (color online). Reflected electric field distribution of the (a) third, (b) fifth, (c) seventh, and (d) ninth harmonics in the $z-y$ plane at $x = 11$ μm at the same time as that in Fig. 1. More information about the third harmonic propagating is available in the Supplemental Material (the plane in Fig. 1(a) changing with the x position from $x = 10.8\times$ μm to $x = 11.54$ μm with $\Delta x = 0.02$ μm).

the LG_{10} mode. For the transmitted beam, the fundamental field is completely reflected by the high-density foil. Thus, the complicated structure in the $y-z$ plane can be shown.

When an intense linearly polarized laser pulse imprints on a solid foil, the foil surface oscillates with double frequency of the incident pulse since the ponderomotive force it feels is $\propto(1-\cos(2\omega_0 t))$, where ω_0 is the incident laser frequency. HHG in both reflected and transmitted beams occurs when the driving beam is a fundamental Gaussian pulse, that is, the LG_{00} mode, which has been elucidated clearly with the simple well-known oscillating mirror model [21–27]. However, in the present case, the oscillating mirror driven by the low-order vortex beam becomes a "vortex oscillating mirror" (VOM). On one side, the mirror is oscillating in the longitudinal direction; on the other side, it is helical in the azimuthal direction transferred from the driving beam. The phase of harmonics radiated from this VOM changes accordingly. The reflected field can be expressed by

$$E \sim a_0 \sin\left(\omega_0 t + l\phi + \kappa \sin(2(\omega_0 t + l\phi))\right), \qquad (2)$$

where κ is related to the oscillating amplitude. After the Fourier expansion of Eq. (1), we can obtain

$$E/a_0 \sim \sum_{n=0}^{\infty} J_n(\kappa) \sin\left((2n+1)(\omega_0 t + l\phi)\right), \qquad (3)$$

where J_n is the first kind of Bessel function. From Eq. (2), we can see that the reflected field indeed includes odd order harmonics just like previous studies of solid HHG. However, the most important is the phase of the harmonic scales with its harmonic order. The topological charge of the m-order harmonic is lm. For example, the mode of the third harmonic should be LG_{30}-like when $l=1$. In another point of view, in the nonlinear process of HHG, a photon of the m-order harmonic is transformed from m photons of the fundamental light carrying the OAM of $\hbar$ per photon. Therefore, the OAM of $m\hbar$ per photon is carried for the m-order harmonic in terms of energy and momentum conservations.

According to the definition of the lm-order azimuthal mode, the phase changes lm times from 0 to 2π in one annular loop in a fixed transverse plane; that is, one annular loop contains $2lm$ intensity (field) peaks. Therefore, the angle between the two adjacent intensity peaks is π/lm, and the angle differences between the intensity peaks of the third and fifth orders, fifth and seventh orders, seventh and ninth orders, and lm order and $(lm+2)$ order in the transverse intensity plane are $2\pi/15$, $2\pi/35$, $2\pi/63$, and $2\pi/lm(lm+2)$, respectively. This result agrees with the display in Fig. 2.

Figure 3(a) shows the intensity profiles of the different harmonics in the transverse direction, which are also the intensity profiles of their corresponding modes. The typical donut distribution of the LG_{l0}-like mode can be clearly observed. For example, the LG_{30} mode of the third harmonic beam is shown in Fig. 3(b). Here, we should note the obtained intensity radius in the transverse direction for different modes keeps the same with that of the driving pulse, shown in Fig. 3(a), which may be slightly different from the standard high-order LG_{l0} mode, in which the transverse radius increases with the mode order. The reason is that the phase term (l) is dominant during the HHG process as analyzed in Eqs. (1) and (2). There may be high-order radical modes in the harmonics which are related to the radical term (p), but it seems they are not dominant since there is mainly one radical ring ($p=0$). Considering the modes we obtained are not standard LG_{l0} modes, strictly speaking, we call them LG_{l0}-like modes. Nonetheless, the azimuthal modes ($l=1,3,5,7,\ldots$) have been indeed induced accompanying the HHG process, which can be seen clearly from the intertwined helices showing the phase components in the field distribution in Fig. 2. Figure 3(c) gives the scaling of the harmonic spectrum with intensity and the conversion efficiency of different modes (harmonics). The spectrum roll-off is fitted by $I_\omega \sim \omega^{-2.98}$, which agrees well with that from the oscillating mirror model or the improved "spiky" mirror model [25]. In the present study, the energy conversion efficiency from the driving LG_{10} pulse to the high-order mode LG_{l0}-like pulse is as high as that of the general solid HHG mechanism. For example, approximately 3% energy of the driving pulse is transferred to the LG_{30}-like mode. This energy is expected to be increased with increasing driving pulse intensity.

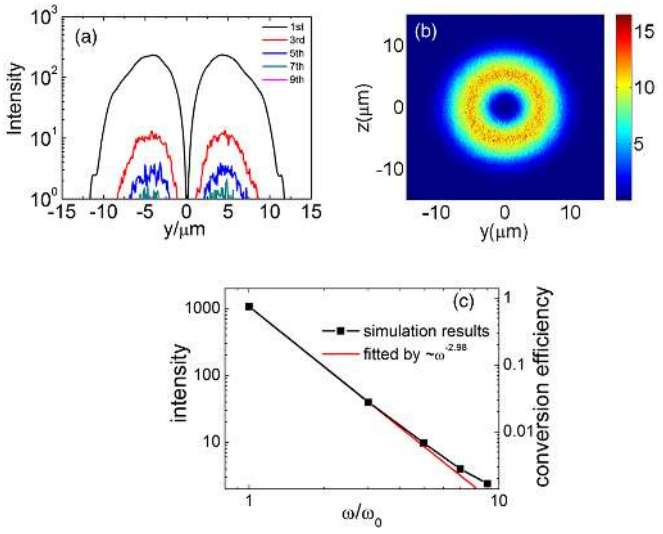

FIG. 3 (color online). (a) Transverse intensity profiles of the fundamental, third, fifth, seventh, and ninth harmonics with the position $y(z)$. (b) Transverse intensity distribution of the third harmonics of LG_{30}-like mode. (c) Harmonic spectrum and conversion efficiency distributions of different modes. The intensity in (a)–(c) is normalized to $(m_e\omega_0 c/e)^2$ and the time is the same as that in Fig. 1.

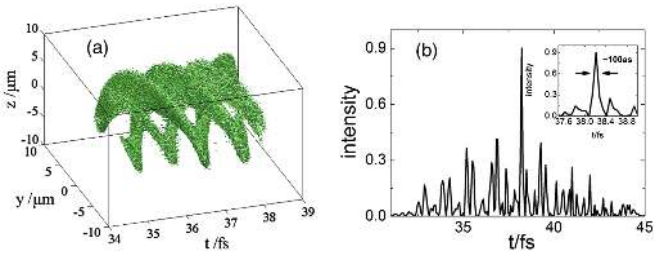

FIG. 4 (color online). (a) Isosurface distribution of the high harmonic field after the fundamental part has been filtered with isosurface value $0.025 m_e \omega_0 c/e$ and (b) its detailed attosecond train structure at the azimuthal angle $\phi = 0°$ ($y = 5$ μm, $z = 0$ μm). The intensity in (b) is normalized to $(m_e \omega_0 c/e)^2$ and the time is the same as that in Fig. 1.

In the spatial scale, we can obtain intense high-order optical vertices, such as LG_{30}-like, LG_{50}-like, LG_{70}-like, and LG_{90}-like beams, and even higher order vertices with fine transversal structures. Conversely, the obtained intense vortex beam may have a fine longitudinal structure in the temporal scale when plasma is used as the ideal nonlinear medium to generate high-order harmonics. As shown in Fig. 4, the helical attosecond pulse (~100 as) train is obtained. Figure 4(a) shows the temporal evolution of a short part field of the whole reflected pulse when the fundamental frequency part is filtered. From this, the helical structure of the harmonics field can be discriminated clearly. Figure 4(b) shows the intensity distribution of the harmonics pulse detected at the positon of $y = 5$, $z = 0$ μm, from which many intensity peaks (an attosecond pulse train) can be seen. These helical attosecond structures may be powerful tools in high-resolution indispensable fields. With the combined characteristics of ultrashort pulse and OAM, these intense attosecond XUV optical vortices will also open a new view for applications in particle micromanipulation imaging [28], optical communication [29,30], and so on.

The scaling relation between the mode and the order of the harmonics agrees well with the above analysis result. According to the relation in Eq. (2), it is possible to get high-order vortices carrying large OAM in the XUV region. The OAM carried per photon is $lm\hbar$, which can make a huge mechanical torque when it interacts with matter. The huge torque is expected to be applied widely, just like the ponderomotive force of the relativistic laser pulse [31]. In the present mode, the redshifting induced by the surface moving ahead into the propagating direction is not considered. We know the driving laser intensity can be scaled to 10^{21} W/cm^2 [32] using plasma as the nonlinear medium to generate ultrashort pulses. If the laser pulse is ultrarelativistic, the redshifting effect is heavy and should be included. That complicated case is beyond of our consideration in this Letter.

In conclusion, we presented a novel scheme to obtain intense high-order vortices in the high frequency region by irradiating a vortex pulse with a low mode on a solid foil. Different from the generation methods with conventional mode transmission related with optical glass, which has a low damage threshold, and the nonlinear process in gas requiring an appropriate ($\sim 10^{14-15}$ W/cm^2) intensity laser pulse, the proposed scheme uses the plasma as the nonlinear medium, which can bear relativistic laser intensity. VOM is formed when the solid plasma is irradiated by an optical vortex beam and radiates high harmonics carrying large OAM with high efficiency. The generated high-order optical vortices exert a strong coherent effect, and the mode of the harmonic scales with the harmonic order and the modes of harmonics (LG_{30}-like, LG_{50}-like, LG_{70}-like, and LG_{90}-like) keep well. According to the reports that other order (even and odd) harmonics can be generated when the laser pulse irradiates obliquely [22,25], other order vertices besides the odd order would be expected since the mode is related to the harmonic order. Given the combined properties of OAM and HHG, the obtained intense vortex beam shows extraordinary applications in both temporal and spatial scales. The intense light beam carrying large OAM is pivotal for its applications in wide and deep fields since a new degree of freedom is added. Moreover, theoretically there is nearly no obstacle when up-shifting the generated twisted beams to a much higher order mode (extremely short and more intense domain) because the phase twist is transferred from the driving field with the low-order mode. There are no limitations for the laser intensity, and therefore a much higher order mode is quite possible by increasing the intensity of the input low-order mode.

The generation mechanism of such an intense (relativistic region) vortex beam is based on plasma HHG with a low-order vortex pulse of relativistic intensity. HHG based on solid plasma has already been studied in experiments [25,26,33–35] and therefore it is quite possible to carry out experimental research to generate the intense high-order vertex beam. The only difference between our work and the above mentioned experiments is the incident laser pulse. Actually, as an alternative of the incident pulse, the low-order vortex pulse generated with the recently proposed light fan regime [31] may be applied in the present scheme. As for the measurement of the temporal characteristics and OAM of the harmonics from the scheme, some alternative methods such as laser-assisted XUV photoionization together with photoelectron spectroscopy [36] or a flat-field EUV spectrometer [32] and a reference beam (by interference with a flat-phase reference) [17] could be applied as in the case of the gas harmonics.

This work was supported by the Ministry of Science and Technology of the People's Republic of China (Grants No. 2011DFA11300 and No. 2011CB808104) and the National Natural Science Foundation of China (Grants No. 61221064, No. 11374319, No. 11125526, No. 11335013, and No. 11127901).

*To whom all correspondence should be addressed.
bfshen@mail.shcnc.ac.cn

[1] A. M. Yao and M. J. Padgett, Adv. Opt. Photonics **3**, 161 (2011).
[2] S. Franke-Arnold, L. Allen, and M. Padgett, Laser Photonics Rev. **2**, 299 (2008).
[3] A. Mair, A. Vaziri, G. Weihs, and A. Zeilinger, Nature (London) **412**, 313 (2001).
[4] M. A. Clifford, J. Arlt, J. Courtial, and K. Dholakia, Opt. Commun. **156**, 300 (1998).
[5] B. S. Davis, L. Kaplan, and J. H. McGuire, J. Opt. **15**, 035403 (2013).
[6] A. Afanasev, C. E. Carlson, and A. Mukherjee, Phys. Rev. A **88**, 033841 (2013).
[7] A. Picon, A. Benseny, J. Mompart, J. R. V. de Aldana, L. Plaja, G. F. Calvo, and L. Roso, New J. Phys. **12**, 083053 (2010).
[8] V. Y. Bazhenov, M. V. Vasnetsov, and M. S. Soskin, JETP Lett. **52**, 429 (1990).
[9] E. Hemsing, A. Knyazik, M. Dunning, D. Xiang, A. Marinelli, C. Hast, and J. B. Rosenzweig, Nat. Phys. **9**, 549 (2013).
[10] E. Hemsing, P. Musumeci, S. Reiche, R. Tikhoplav, A. Marinelli, J. B. Rosenzweig, and A. Gover, Phys. Rev. Lett. **102**, 174801 (2009).
[11] E. Hemsing, A. Marinelli, and J. B. Rosenzweig, Phys. Rev. Lett. **106**, 164803 (2011).
[12] U. D. Jentschura and V. G. Serbo, Phys. Rev. Lett. **106**, 013001 (2011).
[13] P. F. Lan, P. X. Lu, W. Cao, and X. L. Wang, Phys. Rev. A **76**, 043808 (2007).
[14] E. Goulielmakis, M. Schultze, M. Hofstetter, V. S. Yakovlev, J. Gagnon, M. Uiberacker, A. L. Aquila, E. M. Gullikson, D. T. Attwood, R. Kienberger, F. Krausz, and U. Kleineberg, Science **320**, 1614 (2008).
[15] X. M. Feng, S. Gilbertson, H. Mashiko, H. Wang, S. D. Khan, M. Chini, Y. Wu, K. Zhao, and Z. H. Chang, Phys. Rev. Lett. **103**, 183901 (2009).
[16] M. Zurch, C. Kern, P. Hansinger, A. Dreischuh, and C. Spielmann, Nat. Phys. **8**, 743 (2012).
[17] G. Gariepy, J. Leach, K. T. Kim, T. J. Hammond, E. Frumker, R. W. Boyd, and P. B. Corkum, Phys. Rev. Lett. **113**, 153901 (2014).
[18] C. Hernandez-Garcia, A. Picon, J. San Roman, and L. Plaja, Phys. Rev. Lett. **111**, 083602 (2013).
[19] S. Patchkovskii and M. Spanner, Nat. Phys. **8**, 707 (2012).
[20] See Supplemental Material at http://link.aps.org/supplemental/10.1103/PhysRevLett.114.173901 for distributions of reflected E_y of the third harmonic in the $z-y$ plane changing with x.
[21] S. V. Bulanov, N. M. Naumova, and F. Pegoraro, Phys. Plasmas **1**, 745 (1994).
[22] R. Lichters, J. MeyerterVehn, and A. Pukhov, Phys. Plasmas **3**, 3425 (1996).
[23] S. Gordienko, A. Pukhov, O. Shorokhov, and T. Baeva, Phys. Rev. Lett. **93**, 115002 (2004).
[24] T. Baeva, S. Gordienko, and A. Pukhov, Phys. Rev. E **74**, 046404 (2006).
[25] U. Teubner and P. Gibbon, Rev. Mod. Phys. **81**, 445 (2009).
[26] B. Dromey, M. Zepf, A. Gopal, K. Lancaster, M. S. Wei, K. Krushelnick, M. Tatarakis, N. Vakakis, S. Moustaizis, R. Kodama, M. Tampo, C. Stoeckl, R. Clarke, H. Habara, D. Neely, S. Karsch, and P. Norreys, Nat. Phys. **2**, 456 (2006).
[27] N. M. Naumova, J. A. Nees, and G. A. Mourou, Phys. Plasmas **12**, 056707 (2005).
[28] M. Padgett and R. Bowman, Nat. Photonics **5**, 343 (2011).
[29] J. Wang, J. Y. Yang, I. M. Fazal, N. Ahmed, Y. Yan, H. Huang, Y. X. Ren, Y. Yue, S. Dolinar, M. Tur, and A. E. Willner, Nat. Photonics **6**, 488 (2012).
[30] X. L. Cai, J. W. Wang, M. J. Strain, B. Johnson-Morris, J. B. Zhu, M. Sorel, J. L. O'Brien, M. G. Thompson, and S. T. Yu, Science **338**, 363 (2012).
[31] Y. Shi, B. F. Shen, L. G. Zhang, X. M. Zhang, W. P. Wang, and Z. Z. Xu, Phys. Rev. Lett. **112**, 235001 (2014).
[32] F. Dollar, P. Cummings, V. Chvykov, L. Willingale, M. Vargas, V. Yanovsky, C. Zulick, A. Maksimchuk, A. G. R. Thomas, and K. Krushelnick, Phys. Rev. Lett. **110**, 175002 (2013).
[33] U. Teubner, K. Eidmann, U. Wagner, U. Andiel, F. Pisani, G. D. Tsakiris, K. Witte, J. Meyer-ter-Vehn, T. Schlegel, and E. Forster, Phys. Rev. Lett. **92**, 185001 (2004).
[34] Y. Nomura, R. Horlein, P. Tzallas, B. Dromey, S. Rykovanov, Z. Major, J. Osterhoff, S. Karsch, L. Veisz, M. Zepf, D. Charalambidis, F. Krausz, and G. D. Tsakiris, Nat. Phys. **5**, 124 (2009).
[35] C. Thaury, F. Quere, J. P. Geindre, A. Levy, T. Ceccotti, P. Monot, M. Bougeard, F. Reau, P. D'Oliveira, P. Audebert, R. Marjoribanks, and P. H. Martin, Nat. Phys. **3**, 424 (2007).
[36] M. Drescher, M. Hentschel, R. Kienberger, G. Tempea, C. Spielmann, G. A. Reider, P. B. Corkum, and F. Krausz, Science **291**, 1923 (2001).